Atmospheric CO2 Sequestration in Iron and Steel Slag: Consett, County Durham, United Kingdom

William Matthew Mayes,[†] Alex L. Riley,[†,‡] Helena I. Gomes,[†,∇] Peter Brabham,[§] Joanna Hamlyn,[§,∥] Huw Pullin,[§] and Phil Renforth*,[§]

[†]School of Environmental Sciences, University of Hull, Hull HU6 7RX, United Kingdom

[‡]Chemical and Biological Engineering, University of Sheffield, Sheffield S10 2TN, United Kingdom

[§]School of Earth and Ocean Sciences, Cardiff University, Cardiff CF10 3AT, United Kingdom

[∥]TerraDat UK Limited, Penarth Road, Llandough, Cardiff CF11 8TQ, United Kingdom

[∇]Food, Water, Waste Research Group, Faculty of Engineering, University of Nottingham, University Park, Nottingham NG7 2RD, United Kingdom

S Supporting Information

ABSTRACT: Carbonate formation in waste from the steel industry could constitute a nontrivial proportion of the global requirements for removing carbon dioxide from the atmosphere at a potentially low cost. To utilize this potential, we examined atmospheric carbon dioxide sequestration in a >20 million ton legacy slag deposit in northern England, United Kingdom. Carbonates formed from the drainage water of the heap had stable carbon and oxygen isotope values between −12 and −25 ‰ and −5 and −18 ‰ for $\delta^{13}C$ and $\delta^{18}O$, respectively, suggesting atmospheric carbon dioxide sequestration in high-pH solutions. From the analyses of solution saturation states, we estimate that between 280 and 2900 tons of CO_2 have precipitated from the drainage waters. However, by combining a 37 year long data set of the drainage water chemistry with geospatial analysis, we estimate that <1% of the maximum carbon-capture potential of the deposit may have been realized. This implies that uncontrolled deposition of slag is insufficient to maximize carbon sequestration, and there may be considerable quantities of unreacted legacy deposits available for atmospheric carbon sequestration.
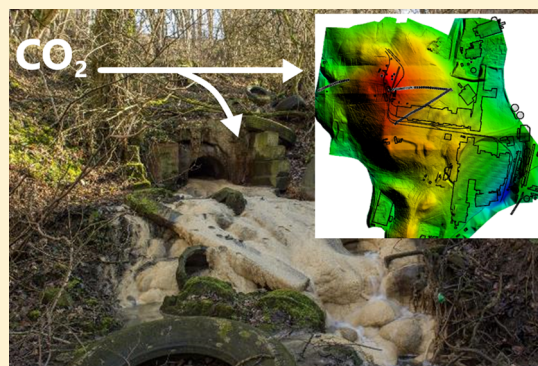
INTRODUCTION

The steel industry produces around half a billion tons of an alkaline material (known as slag) globally each year.[1] Blast furnace slags commonly find uses as secondary aggregate,[2] pozzolan,[3] or agricultural lime.[4] However, due to the higher concentrations of oxides and hydroxides (which may cause expansion if used directly in aggregate), slag from steel production is typically "weathered" for months to years prior to use.[5] While the proportion of slag being reused varies with regional demand, a sizable proportion of annual production is ultimately stockpiled in steelworks.[6,7] This, alongside historic deposits of iron and steel slag, creates environmental issues associated with highly alkaline leachates (pH > 11).[8,9] The dissolution of these materials releases calcium and magnesium ions from oxide and silicate minerals and glass and amorphous material, which raises pH beyond that encountered in most natural settings (see eqs 1 and 2, which show dissolution reactions for larnite and portlandite, respectively):

$$Ca_2SiO_4 + 4H_2O \rightarrow 2Ca^{2+} + H_4SiO_4 + 4OH^- \quad (1)$$

$$Ca(OH)_2 \rightarrow Ca^{2+} + 2OH^- \quad (2)$$
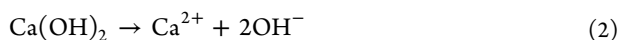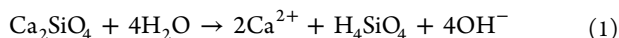
These hydroxide-enriched leachates promote the dissolution of atmospheric carbon dioxide (CO_2) into solution, which reacts to form carbonate and bicarbonate ions (eq 3). Slag leachates are rich in dissolved calcium (Ca), which leads to the supersaturation of calcium carbonate minerals (e.g., calcite) and rapid rates of precipitation of secondary carbonates (eq 4).[10,11] Such leachates can pose enduring[12] and acute[13] environmental issues due to the physical smothering ("armoring") of receiving streams alongside extreme pH and potential metalloid enrichment and mobility.[14−16] However, carbonate precipitation buffers the waters back toward circumneutral pH, which limits metalloid solubility:
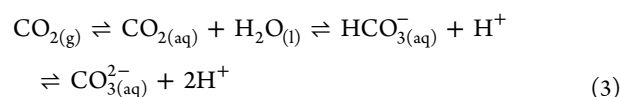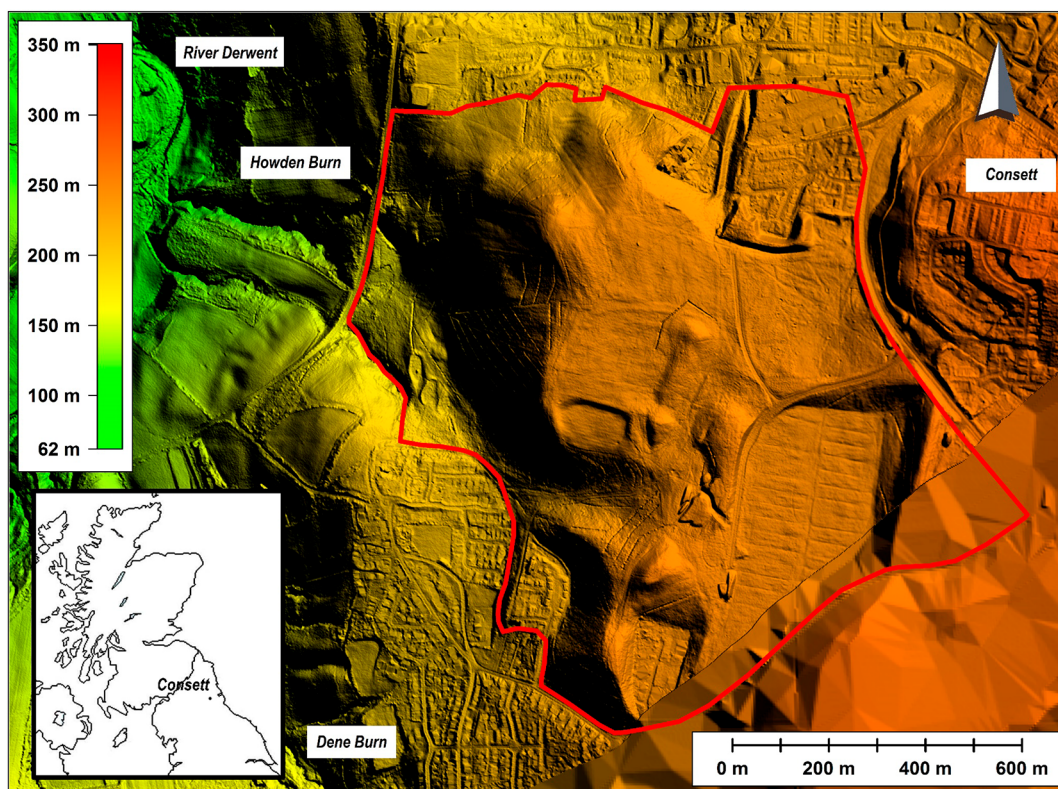
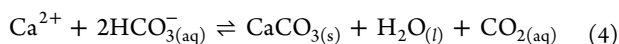$$CO_{2(g)} \rightleftharpoons CO_{2(aq)} + H_2O_{(l)} \rightleftharpoons HCO_{3(aq)}^- + H^+$$
$$\rightleftharpoons CO_{3(aq)}^{2-} + 2H^+ \quad (3)$$

Figure 1. Location map showing the topography of the former Consett Steelworks drainage systems. The color scale represents the elevation above sea level derived from 1 and 5 m LIDAR data.[32] The red line denotes the boundary of the study site.

$$Ca^{2+} + 2HCO_3^-_{(aq)} \rightleftharpoons CaCO_{3(s)} + H_2O_{(l)} + CO_{2(aq)} \quad (4)$$

The potential for steel slags to capture atmospheric CO_2 in the form of stable carbonates has been extensively studied, initially in reaction vessels at elevated temperatures (>200 °C) and enriched CO_2 gas concentrations (>10%) and pressures (~20 bar),[17−21] with a theoretical CO_2 sequestration capacity of 0.27 to 0.43 kg CO_2 per kilogram of slag (see Supporting Information S1). This capacity can be improved through the application of "enhanced weathering",[22,23] which is an alternative CO_2 sequestration pathway in which carbon is stored as dissolved bicarbonate in the ocean.[24] In this approach, almost twice as much CO_2 may be sequestered (eq 5):

$$Ca_2SiO_4 + 4H_2O + 4CO_2 \rightarrow 2Ca^{2+} + H_4SiO_4 + 4HCO_3^- \quad (5)$$
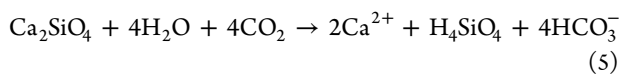
The removal of CO_2 from the atmosphere ("negative emissions" or "greenhouse gas removal") is emerging as an important policy requirement for limiting global temperature change of <2 °C.[25,26] Emission-reduction scenarios predicted to achieve this require between 180 and 900 Gt CO_2 to be removed from the atmosphere over the coming century[27] alongside limiting further emissions. Atmospheric carbon sequestration in the steel industry may provide a relatively cheap method of negative emissions and, in the case of carbonate formation, a means for waste remediation.[28] The removal of atmospheric CO_2 into waste materials has previously been explored in chrysotile mine tailings (e.g., ref 29) in soils mixed with concrete from demolition.[30,31] To constrain the potential of CO_2 sequestration in waste from the steel industry, we quantify atmospheric carbon sequestration in

a deposit of slag associated with an iron and steel works that closed nearly four decades ago.

■ MATERIALS AND METHODS

Study Site. For over 100 years, an iron and steel works located in Consett, County Durham, U.K. produced cumulatively around 120 million tons of iron and steel. This led to the creation of >20 million of tons of slag, which was deposited in several large mounds adjacent to the works. Production ceased in 1980, and the heaps were landscaped and capped with thin clay topsoil and have been passively managed (Figure 1). The deposits are underlain by alluvium and glacial till overlying carboniferous coal measures, and the largest deposit was heaped over a partially culverted watercourse (the Howden Burn), which receives the bulk of the drainage water. A smaller heap is located to the south of the main workings (Figure 1), the drainage waters of which collect in a pond before discharging through a naturally developed wetland in the Hownsgill Valley and into a watercourse (the Dene Burn)[9] (see Supporting Information S2 for location and site details).

Volume Estimates. LIDAR data[32] (resolution of 2 and 5 m) were compiled for the site, representing the modern ground surface. A total of 41 spot heights were recorded from the historic 1890 Ordnance Survey map and used to create a low-resolution 5.3 km² digital elevation model of the natural ground surface underlying the site. The comparison between these two digital elevation models was used to estimate the volume of the northern heap (estimation completed using the terrain subtraction function in Global Mapper v18 1.0; see Supporting Information S3).

Resistivity Tomography Survey. The depth of the slag deposit has been confirmed using electrical resistivity
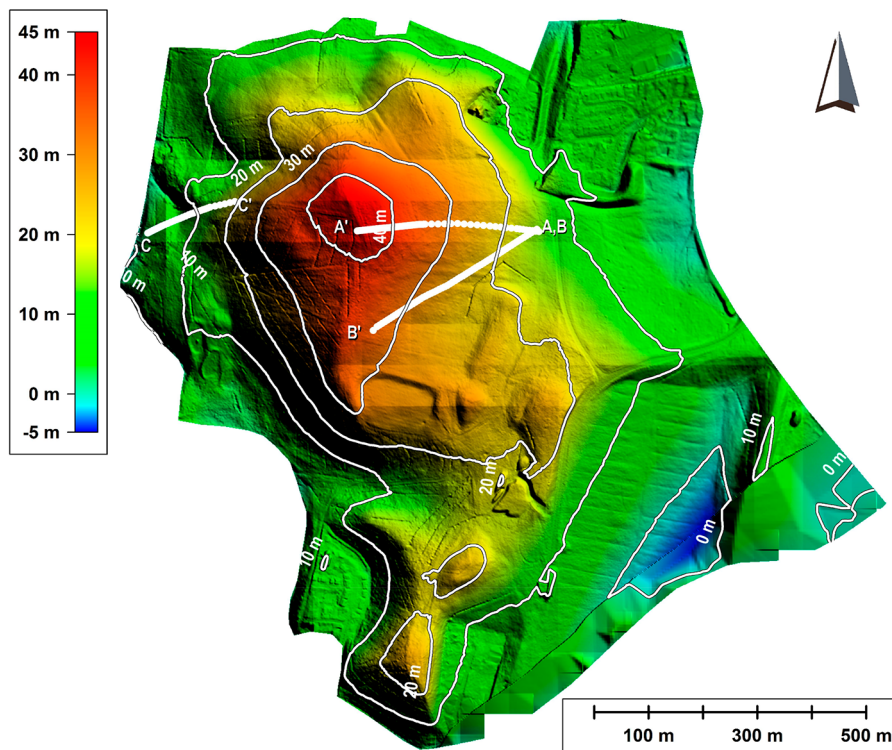
Figure 2. Estimate of the depth of the slag deposit based on the comparison of pre- and post-deposit digital elevation models. The bold white lines (A/A′, B/B′, and C/C′) represent the locations of the resistivity survey (see Figure 3).

tomography (ERT) surveys, which determined the depth of the contact between the slag and the underlying natural ground. A 72-channel IRIS Syscal resistivity system was used to acquire three profiles (A, B, and C) across the slag deposits (shown in Figure 2). Profiles A and B transect the top of the slag deposit to observe how slag thickness increases with distance away from the side of the valley; profile B strikes toward the foundations of the now-demolished steel work buildings (see the Supporting Information). Profile C trends from the bottom of the slag deposit toward profile A. Profiles A and B were acquired with a 5 m electrode spacing, giving a maximum depth of investigation of ∼50 m below ground level (bgl). ERT Profile C was acquired with an electrode spacing of 2.5 m, giving a maximum depth of investigation of ∼25 m bgl. The data were processed using Res2DInv software to derive modeled electrical cross-sections of the subsurface. The resulting resistivity models for profiles A, B, and C had a root mean square (RMS) error of 8%, 17%, and 9%, respectively. Robust inversion was not used to allow for more geologically realistic results; hence, the higher RMS values were condoned. The finalized models were calculated within four or fewer iterations. The elevation data were added to the models using electrodes positions extracted from LIDAR data (Figure 1). Finally, these data were exported into Surfer 7, gridded, and presented as a 2D cross-section of resistivity.

Chemical Sampling and Analysis. Long-term water-quality records from the site are compiled from monitoring by regulatory agencies (Environment Agency and their predecessor, the National Rivers Authority) that routinely sampled major physicochemical parameters, major ions, and minor elements from 1978−2000. However, sample collection was sporadic, ranging from monthly to annual sampling in frequency. From 2004 onward, annual sampling (as a minimum) has been undertaken by the authors at the same

locations in the Howden and Dene Burns. Bimonthly samples were collected from the Hownsgill valley wetland between 2004 and 2006,[9] and ad-hoc samples were collected up to 2015. Field sampling consisted of major labile variables (pH, electrical conductivity, Eh, and temperature using a Myron Ultrameter) and total alkalinity, which was measured in situ using a Hach digital titrator (0.8 mol/L H_2SO_4 with bromocresol green−methyl blue indicator). Samples were also taken in acid-washed high-density polyethylene bottles for field-filtered (0.45 μm) samples, which were acidified with trace-metal-grade HNO_3 and analyzed for major cation content using a PerkinElmer Optima 5300 DV inductively coupled plasma optical emission spectrometer.

Long-term patterns in saturation index for calcite were determined using the geochemical code PHREEQC[33] with the Lawrence Livermore National Laboratory database based on sample dates for which synchronous pH, temperature, Ca and total alkalinity data were available. Trends in calcite saturation index ($SI_{calcite}$) for the Dene Burn and Howden Burn are assessed using Partial Mann−Kendall tests with flow as a covariate (as per ref 12). Flow at the time of sampling was either manually measured or determined from an adjacent permanent flow gauging station (River Derwent at Rowlands Gill, National River Flow Archive station: 23 007) adjusting for the catchment area (see Supporting Information S2).

Synchronous sampling for water quality and flow along the courses of the Dene Burn and Howden Burn was undertaken from 2003 to 2015 on 14 and 8 occasions, respectively. The Hownsgill Valley wetland was sampled on 10 occasions from 2004 to 2006.[9] This enables the determination of mass loss of Ca between successive downstream sample locations (the mass load being the product of flow and concentration) from which to assess carbonate precipitation rate, assuming that all Ca load lost from the water column is as $CaCO_3$ (eq 4). A source
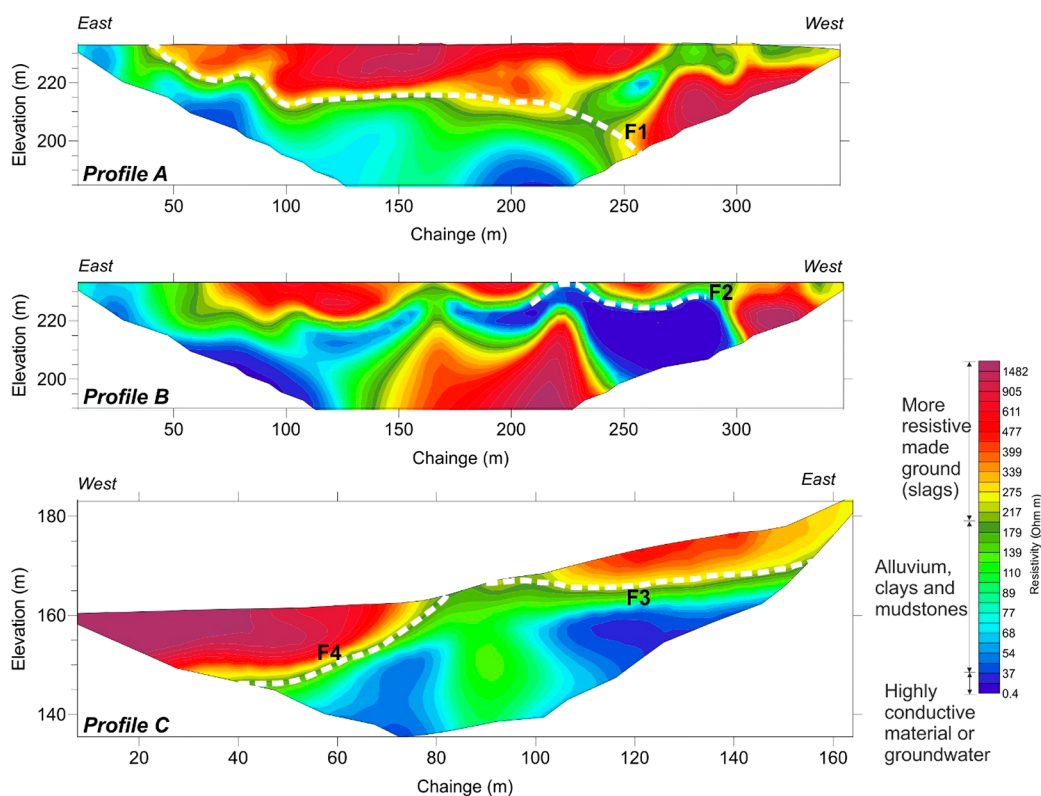
Figure 3. Results from the electrical resistivity tomography. Location of the lines are presented in Figure 2. Transition between high and low resistivity potentially denote changes in ground conditions (e.g., between slag and the natural ground in F1 and F3).

location and downstream location (in between which there were no major tributaries) along the course of each stream were sampled for major physicochemical parameters as above. Flow was measured using a Valeport 801 velocity meter with a flat sensor suited to the shallow stream depths (typically <0.2 m) via the velocity area method. The length of the channel reaches was determined through measurement in ArcGIS version 10 of 1:1000 Ordnance Survey base maps.[34] Average channel width was taken from manual spot measurements of channel width every 50 m of the study reaches. The area of the Hownsgill Valley wetland was determined by a manual field survey with a differential GPS.[9] Synoptic sampling was undertaken over a range of flow conditions from which relationships between source chemistry (notably $SI_{calcite}$) can be related to the estimated mass of carbonates deposited on the downstream streambed (eq 6):

$$P = 2.5\left(\frac{Q_d(C_s - C_d)}{A}\right) \quad (6)$$

where P is the area adjusted calcium carbonate precipitation rate (g/m^2/day); Q_d equates to the mean daily flow rate (m^3/day); C_s is the Ca source concentration (mg/L); C_d is the concentration of Ca at downstream sample location (mg/L); and A is the stream area (m^2) based on length of reach (geographic information system derived) and average width from the spot measurements. The multiplier is the ratio between the molar mass of Ca and $CaCO_3$.

A series of 14 surficial secondary carbonate samples were taken from the streambeds of the Howden and Dene Burns alongside samples from carbonate hardpans in the Hownsgill Valley wetland (see Supporting Information S5). The samples were crushed using an agate pestle and mortar and analyzed for

stable carbon and oxygen isotope ratios using a Kiel IV carbonate device calibrated against a Vienna Pee Dee belemnite standard. The standard error for the analysis is 0.001 ‰ and 0.003 ‰ for δ^{13}C and δ^{18}O, respectively. To this powder, ultrapure acetone was added, and the resultant slurry was pipetted onto a clean glass slide. The slides were allowed to dry and then analyzed using a Philips PW1710 automated powder diffractomer with a CuK radiation source operating at 35 kV and 40 mA. Samples were scanned from 2 to 70 °2θ at a step size of 0.02 °2θ with a counting time of 1 s per step. Diffraction patterns were analyzed using PW1876 PC-Identify software (version 1.0b) and compared with the JCPDS cards of standard materials.

■ RESULTS AND DISCUSSION

Volume Estimates and Resistivity Tomography. By the creation and comparison of elevation models of the current (from LIDAR data) and pre-slag (from spot heights of historic maps) terrain, it is possible to estimate the depth of the deposit and the total volume of the material (Figure 2). The analysis suggests depths of the largest deposit range up to 45 m, which is consistent with historic accounts of the site[35,36] and that the total volume of material is ~16 Mm^3, which is consistent with theoretical maximum historic production estimates (see Supporting Information S6). Given that the bulk density of slag is typically between 1 and 1.5 Mg/m^3[37] and that the concentration of CaO and MgO is between 34 and 42% and 8 and 12% by mass, respectively,[38] then the carbon dioxide sequestration potential for the largest heap is 6−11 million tons of CO_2 (as mineral carbonate) or 10−19 million tons of CO_2 (through enhanced weathering).

The results of the ERT geophysical surveys are shown in Figure 3. The interpretation for each technique is obtained by comparison with known values of common materials.[39] Each ERT profile shows a more resistive material overlying a more-conductive material. In this scenario, the slag deposits are more resistive than the underlying natural geology, which is composed of alluvium, clays, and mudstones. This may be due to a well-drained slag overlying saturated natural ground or that the conductive metals contained in the slag are fixed within a silicate matrix, creating a more-resistive material than the natural ground. Profile A shows an undulating boundary (feature F1) between more-resistive and more-conductive material that begins at ground level, goes 50 m along the profile, and deepens to the west. The authors interpret this as the boundary between the slag and natural ground. Profile A also shows a shallow, less-resistive feature that may be related to groundwater flow. Profile B shows a highly heterogeneous image of resistivity; the very-low-resistivity feature (F2) is likely to be a plume of highly conductive groundwater caused by solutes within the slag. Profile C shows a clear boundary between a more-conductive underlying geology and a more-resistive overburden. Feature (F3) is likely to represent the boundary between the slag deposit and the underlying geology. The boundary on the west side of the profile (F4) is caused by made ground due to a nearby road and is not related to the slag deposit.

Stream Water Geochemistry. A total of three drainage streams at the site are characterized by hyperalkaline pH (typically in the range 10 to 12.5 at source), dominated by $Ca-OH-SO_4$ waters (see Supporting Information S7), where the sulfur potentially originates from the coke or coal used in the blast furnace. All drainage streams are consistently supersaturated with a range of carbonate phases (Supporting Information S7), with calcite being dominant in the extensive downstream secondary deposits (see Figure S11). As such, long-term changes in aqueous chemistry focus on saturation indices for calcite hereafter (Figure 4). Flow in each of the systems is relatively steady, receiving a mixture of groundwater from within the slag or spring water from the underlying coal measures[11] generally rich in Ca, which are occasionally diluted by solute-poor surface runoff (Supporting Information S7).[11,12]

There has been a slight change in bulk drainage chemistry in 37 years of monitoring. There was a significant decline in saturation index in waters draining to the Dene Burn (Figure 2A; PMK: −856; P = 0.002) irrespective of flow condition, which showed no significant long-term trend (PMK: 220; P = 0.421). This may be indicative of gradual exhaustion of alkalinity generating minerals (e.g., Ca silicates, free lime, or portlandite) in the slag deposits with weathering (see Supporting Information S7).[12] No significant trend in $SI_{calcite}$ or flow in the Howden Burn is apparent (Figure 2B; $SI_{calcite}$: PMK: 9.3: P = 0.80; flow: PMK: 22; P = 0.95), although a clear decline and then subsequent recovery in $SI_{calcite}$ is apparent between the mid-1980s and the early part of the 21st century, respectively. This has previously been attributed to changes in flow paths and significant groundwork in this subcatchment as part of broader restoration works.[12] The Howden Burn drains a much greater proportion of the slag deposits at the site ($>^3/_4$ of the total area and much greater depths) than the Dene Burn. As such, it may explain why there has been no sign of decline in alkalinity generation yet in the Howden Burn. Regardless of temporal changes, the $SI_{calcite}$ in
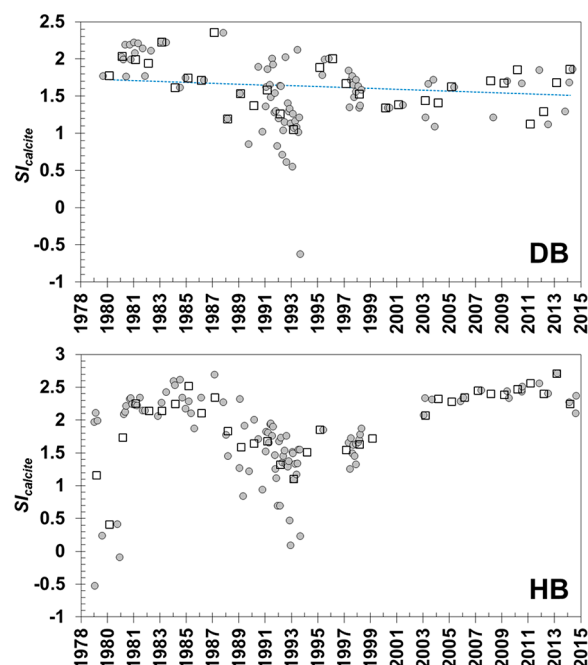

Figure 4. Long-term calcite saturation index ($SI_{calcite}$) values for the Dene Burn (DB) and Howden Burn (HB). Closed gray circles show individual measurements; open squares show averages for each hydrological year (October 1−September 30). The blue trend line in the upper plot (Dene Burn) based on the Sen's slope statistic shows the significant decline in $SI_{calcite}$ from the partial Mann−Kendall Tests (see the text). No significant trend was apparent in the Howden Burn (lower plot).

all systems is typically in a range in which spontaneous calcium carbonate precipitation would be anticipated (>+0.3) and generally above +1.5, at which point homogeneous precipitation is expected[40] (see Table S2).

Evidence of Carbonate Precipitation. Observations of calcium carbonate precipitation are common in the drainage waters emanating from slag deposits[8] and provide a means for translating the long-term saturation index data into carbon mass balances for the drainage streams. The mass loss of Ca between source and a downstream sample location is divided by reach area (eq 6). The synoptic sampling of the receiving streams at Consett reveals a strong and significant positive relationship (Spearman r_s: 0.82; p < 0.001; ANOVA regression of F: 52.1; p < 0.001) between empirical estimates of $CaCO_3$ precipitation rate and $SI_{calcite}$ at the source of the discharge (Figure 5). The higher $CaCO_3$ precipitation rates are apparent in the Howden Burn with a range of 8−259 g/m^2/day, where waters are typically further from equilibrium (see the higher $SI_{calcite}$ values in Table S2) as compared to the Dene Burn (range 7−116 g/m^2/day: Table 1), which has lower $SI_{calcite}$ values.

Precipitation rates across the wetlands that receive leachate in the Hownsgill Valley have been previously published, based on intensive monitoring of aqueous geochemistry,[9,30] and are in the range of 1 to 10 g/m^2/day (Table 1). These lower rates are readily ascribed to the topographical differences between the Hownsgill Valley wetland, which is low gradient and thus limited by the rate of diffusion of atmospheric CO_2 (in addition to microbially generated CO_2 in the water column and substrate)[9] compared with the cascading Howden and Dene Burns. In the faster-flowing systems, the dissolution rates
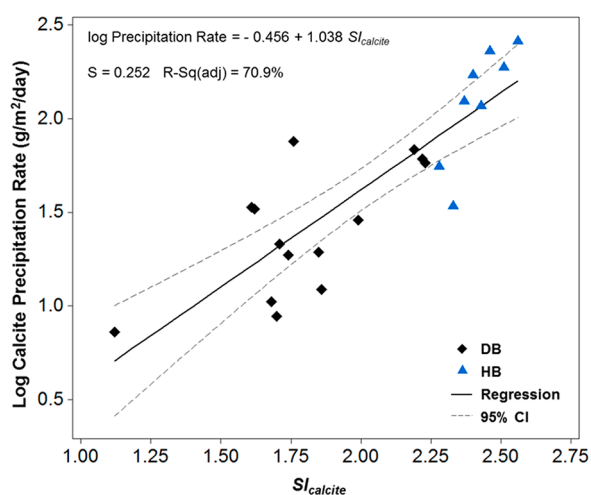
Figure 5. Relationship between $SI_{calcite}$ and empirically observed calcium carbonate precipitation rate (shown as $\log_{10}$ values) across the Dene Burn (DB) and Howden Burn (HB) streams.

Table 1. Estimated Calcium Carbonate Precipitation Rates for the Three Drainage Systems at the Site of the Former Consett Steelworks Derived from Loadings-Based Assessments[a]

	Dene Burn	Howden Burn	Hownsgill Valley
area between sample locations (m^2)	2310	525	2863
n	14	8	10
Ca^{2+} load loss (kg/day)	28.4 (6.7–107.6)	30.9 (1.7–54.4)	6.2 (1.2–10.9)
$CaCO_3$ precipitation rate (g/m^2/day)	31 (7–116)	147 (8–259)	5 (1–10)

[a]Flux data show median and the range in parentheses.

of CO_2 into solution are likely to be far greater given the turbulent flow of the shallow waters over secondary carbonate barrage cascades (see Supporting Information S4).[41]

Carbonate Deposit Analysis. Stable carbon and oxygen isotope ratios have been widely used to assess provenance of carbonate minerals (e.g., ref 42). Carbonates formed from highly alkaline solutions derived from the dissolution of steel slags, lime waste, cement wastes, or alkaline mine tailings[30,43,29] have very characteristic negative $\delta^{13}C$ isotopic signatures.[30,44,45] These have been ascribed to a stable carbon isotopic enrichment factor ($\varepsilon_{CaCO_3-CO_2} = -19$ ‰) in carbonate and dissolved aqueous CO_2 from the reaction between aqueous CO_2 and hydroxide ions ("hydroxylation").[46] The isotopic value of oxygen in carbonate minerals formed from high-pH solutions is a mixture of the isotopic value of hydroxide ions and atmospheric CO_2.[46−48] This fractionation gives rise to the highly negative $\delta^{18}O$ isotope values (−24 and −19 ‰) characteristic of hyperalkaline sites (eg., cements[30,49,50] and hyperalkaline groundwater).[51] The use of isotopic values unambiguously demonstrates incorporation of atmospheric CO_2 into solid carbonate minerals.

The stable carbon and oxygen isotope ratios for the deposits in the three drainage streams at Consett are presented in Figure 6. The more-negative $\delta^{13}C$ and $\delta^{18}O$ values were recorded in samples from the Howden Burn and Hownsgill Valley, where dilution of the leachate by uncontaminated ground or surface waters was minimal.[11] The Dene Burn,
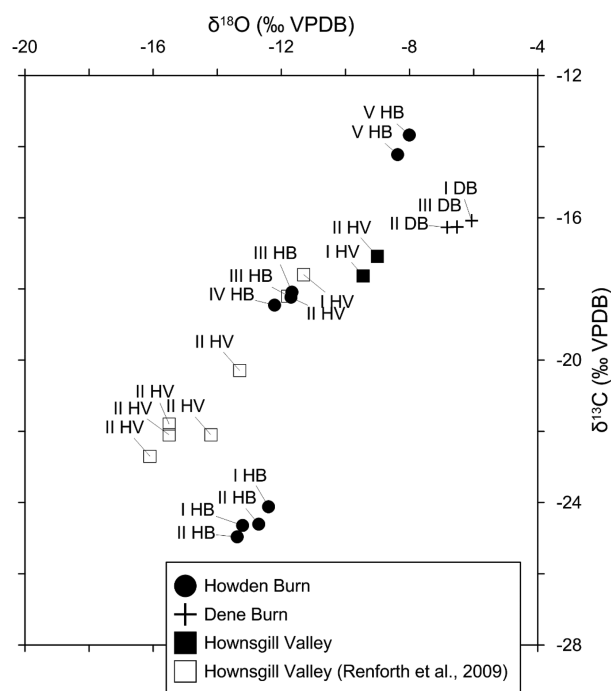
Figure 6. $\delta^{18}O$ and $\delta^{13}C$ values of carbonates formed in the drainage waters of the slag heaps at Consett, County Durham.

which receives drainage rising from a spring line in the Coal Measures (rich in bicarbonate),[52] has the least-negative $\delta^{13}C$ and $\delta^{18}O$ values. A common approach to assessing the relative portion of atmospheric CO_2 in the secondary mineral deposits produced from highly alkaline solutions is via the use of a linear mixing model that assumes carbon in a mineral sample is sourced from two end-member reservoirs (e.g., ref 53). If atmospheric CO_2 is the only source of carbon in hydroxylation isotopic fractionation, the proximity of the isotope values in the samples to end members can be used to determine the quantity of sequestered atmospheric CO_2 in the secondary deposits. Hydroxylation will produce an end member with an isotopic ratio of −25.3 ‰ for $\delta^{13}C$; see ref 31). Therefore, based on the proximity of the data in Figure 6 to a "lithogenic" ($\delta^{13}C = 0$ ‰) and the "hydroxylation" end members, it is estimated that between 54% and 99% of the carbon in the carbonate is derived from the atmosphere, and the remaining carbonate is derived from lithogenic sources.

Carbon Budget and Storage Potential. The drainage water chemistry and flow suggests that approximately 314 tons of calcium have been leached from the heaps over the past 37 years, which is approximately >0.004% of the potentially available calcium based on the volume and typical composition of slag.[16] Even if the same concentration of calcium was present in the drainage waters since the rapid expansion of the heaps in the early 1900s (~8.5 tons per year) and the flow through the site was similar to present levels, approximately 850 tons of calcium would have been leached over 100 years. Estimates of carbonate precipitation from stream waters suggest that between 281 and 2890 tons of CO_2 have been sequestered since the work's closure in 1980 (Table 2). For comparison, this equates to approximately 255−2627 tons of calcium; the upper value is consistent with calcium leaching values. Given that the heaps may contain 3.9−7.2 million tons of calcium, only a very small proportion has been leached, and

Table 2. Total Carbon-Flux Estimates Based on Long-Term SI$_{calcite}$ Data, Empirical Loading Measurements, and Isotopic Characterization of Secondary Deposits[a]

site	average CaCO$_3$ formation in drainage waters (ton/year)	%CO$_2$ from atmosphere	average atmospheric CO$_2$ uptake (ton/year)	total CO$_2$ tons (1978–2015)
Dene Burn	17.6 (5.4–57.1)	64	3.5–36.5	130–1351
Howden Burn	13.0 (4.0–42.1)	80	3.2–33.7	118–1247
Hownsgill Valley	5.7 (1.1–9.9)*	79	0.9–7.8	33–292
total	–	–	–	281–2890

[a]Total estimated low and high range (in parentheses) based on an aggregated margin of error of relationship between SI$_{calcite}$ and precipitation rate (Figure 4) and standard deviation of isotopic characterization. The asterisk indicates Hownsgill Valley calculations based on the minimum and maximum recorded average precipitation rates in intensive sampling; long-term total extrapolates were taken from this single year.

the carbon sequestration potential of the material has not been exploited.

The poor conversion of the carbon capture potential may be attributed to limited ingress of atmospheric CO$_2$ into the heap. For instance, if the groundwater inside the heap was in equilibrium with Ca(OH)$_2$, atmospheric CO$_2$, and CaCO$_3$ (and thus precipitating carbonate minerals), waters would have a pH of 10.2 and 0.1 mmol l^{-1} of Ca (see Supporting Information S7 for geochemical modeling). However, the concentration of Ca (∼1–5 mmol l^{-1}) and pH (∼11.5) in the drainage waters is more consistent with the equilibrium concentration ([Ca] ≈ 20 mmol L^{-1}; pH = 12.5) of portlandite (Ca(OH)$_2$) or larnite (Ca$_2$SiO$_4$), which are common minerals in slag.[54] The lower than expected pH and calcium concentration could be caused by dilution of leachate with meteoric or groundwater or a kinetic limitation of weathering (e.g., surface armoring of slag with carbonate or C–S–H phases, limiting weathering rates).[15,17]

Implications. The steel industry is responsible for more than 5% of the total greenhouse gas emissions worldwide,[55] with more than 2 tons of CO$_2$ released per ton of steel manufactured,[19] which equates to over 6 tons of CO$_2$ released for every ton of slag. Slag has the potential to capture ∼0.4 tCO$_2$ per ton as a mineral carbonate or up to 0.7 tCO$_2$ per ton through enhanced weathering. The full carbon cycle of iron and steel slag production and weathering is currently far from a negative-emissions technology and would merely offset emissions from the production site. However, the iron and steel industry will be under increasing pressure to reduce emissions, which may fall to 0.3 tCO$_2$ per ton of steel (0.5 tCO$_2$ per ton of slag), primarily by mixing low carbon fuels into the blast furnace, exploiting a low-carbon power sector, and the capture and geological storage of CO$_2$ emissions.[56] If these emission reductions were achieved, additional carbon sequestration through slag weathering may be sufficient to create an overall carbon negative steel industry. Furthermore, there may be considerable atmospheric removal potential of legacy slag deposits, which are plentiful in many currently steel-producing areas and post-industrial settings. If the requirements of COP21[57] are to be implemented, there is likely to be a requirement for "negative emissions" technologies to keep

atmospheric CO$_2$ within targets.[25,58] Half a billion tons of slag are produced annually,[1] a number that may increase to over a billion tons in the current century. Considering these production values, it is estimated that the industry may be able to remove half a billion tons of CO$_2$ out of the atmosphere per year.

Proactive management of slag to account for, and accelerate, carbon uptake (e.g., through comminution of slag where carbon budgets are favorable) while addressing any potential environmental concern of hyperalkaline discharges on recipient watercourses could provide mutual benefits. Leachate management to minimize subsequent impacts on the aquatic environment is likely to be best addressed via (a) the aeration of waters (e.g., CO$_2$ sparging, the cascading of thin films of leachate over barrages where a hydraulic head is suitable);[10,41] (b) settlement lagoons to allow the accumulation and ready recovery of precipitated calcium carbonates (e.g., ref 59); and (c) residual buffering of alkaline leachates with wetlands.[60,61] In addition to wetland habitat creation as part of broader post-industrial restoration, there may be opportunities, through careful treatment of the leachate, to recover and reuse the high-purity precipitated calcite (potentially used as a filler and coating in paper manufacturing)[18,62] and typically benign in terms of trace element content.[61]

■ ASSOCIATED CONTENT

ⓢ Supporting Information

The Supporting Information is available free of charge on the ACS Publications website at DOI: 10.1021/acs.est.8b01883.

> Tables showing experimental conditions and carbonation potential and major physico-chemical characteristics. Additional details on flow derivation, the method for volume estimation, resistivity tomography survey, historic production, and geochemical data. (PDF)

■ AUTHOR INFORMATION

Corresponding Author
*E-mail: RenforthP@cardiff.ac.uk.
ORCID Ⓞ
Phil Renforth: 0000-0002-1460-9947
Notes
The authors declare no competing financial interest.

■ ACKNOWLEDGMENTS

reviewers, whose comments significantly improved the manuscript. W.M. and P.R. thank Professor Paul Younger posthumously for prompting the initial research at the site many years ago; his vision, insight, and wit will be sorely missed.

■ REFERENCES

(1) USGS. *USGS Minerals Yearbook.* https://minerals.usgs.gov/minerals/pubs/commodity/iron_&_steel_slag/index.html#myb (accessed May 1, 2018].

(2) Ahmedzade, P.; Sengoz, B. Evaluation of steel slag coarse aggregate in hot mix asphalt concrete. *J. Hazard. Mater.* **2009**, *165* (1), 300−305.

(3) Roy, D. M.; ldorn, G. M. Hydration, Structure, and Properties of Blast Furnace Slag Cements, Mortars, and Concrete. *J. Proc.* **1982**, *79* (6), 444−457.

(4) Davis, F.; Collier, B.; Carter, O. Blast-furnace slag as agricultural liming material. *Commer. Fertil.* **1950**, *80* (5), 48−49.

(5) Wang, G. C. *The Utilization of Slag in Civil Infrastructure Construction*; Woodhead Publishing, Elsevier, Duxford, UK, 2016.

(6) Yi, H.; Xu, G.; Cheng, H.; Wang, J.; Wan, Y.; Chen, H. An Overview of Utilization of Steel Slag. *Procedia Environ. Sci.* **2012**, *16* (C), 791−801.

(7) Euroslag. Statistics. http://www.euroslag.com/products/statistics/2014/ (accessed May 1, 2018).

(8) Koryak, M.; Stafford, L. J.; Reilly, R. J.; Magnuson, M. P. Impacts of Steel Mill Slag Leachate on the Water Quality of a Small Pennsylvania Stream. *J. Freshwater Ecol.* **2002**, *17* (3), 461−465.

(9) Mayes, W. M.; Younger, P. L. Buffering of Alkaline Steel Slag Leachate across a Natural Wetland. *Environ. Sci. Technol.* **2006**, *40* (4), 1237−1243.

(10) Roadcap, G. S.; Kelly, W. R.; Bethke, C. M. Geochemistry of Extremely Alkaline (pH > 12) Ground Water in Slag-Fill Aquifers. *Groundwater* **2005**, *43* (6), 806−816.

(11) Mayes, W. M.; Younger, P. L.; Aumônier, J. Hydrogeochemistry of Alkaline Steel Slag Leachates in the UK. *Water, Air, Soil Pollut.* **2008**, *195* (1), 35−50.

(12) Riley, A. L.; Mayes, W. M. Long-term evolution of highly alkaline steel slag drainage waters. *Environ. Monit. Assess.* **2015**, *187* (7), 463.

(13) Hull, S. L.; Oty, U. V.; Mayes, W. M. Rapid recovery of benthic invertebrates downstream of hyperalkaline steel slag discharges. *Hydrobiologia* **2014**, *736* (1), 83−97.

(14) Chaurand, P.; Rose, J.; Briois, V.; Olivi, L.; Hazemann, J.-L.; Proux, O.; Domas, J.; Bottero, J.-Y. Environmental impacts of steel slag reused in road construction: A crystallographic and molecular (XANES) approach. *J. Hazard. Mater.* **2007**, *139* (3), 537−542.

(15) Hobson, A. J.; Stewart, D. I.; Bray, A. W.; Mortimer, R. J. G.; Mayes, W. M.; Rogerson, M.; Burke, I. T. Mechanism of Vanadium Leaching during Surface Weathering of Basic Oxygen Furnace Steel Slag Blocks: A Microfocus X-ray Absorption Spectroscopy and Electron Microscopy Study. *Environ. Sci. Technol.* **2017**, *51* (14), 7823−7830.

(16) Piatak, N. M.; Parsons, M. B.; Seal, R. R. Characteristics and environmental aspects of slag: A review. *Appl. Geochem.* **2015**, *57*, 236−266.

(17) Huijgen, W. J. J.; Comans, R. N. J. Mineral CO2 Sequestration by Steel Slag Carbonation. *Environ. Sci. Technol.* **2005**, *39* (24), 9676−9682.

(18) Eloneva, S.; Teir, S.; Salminen, J.; Fogelholm, C.-J.; Zevenhoven, R. Steel Converter Slag as a Raw Material for Precipitation of Pure Calcium Carbonate. *Ind. Eng. Chem. Res.* **2008**, *47* (18), 7104−7111.

(19) Yu, J.; Wang, K. Study on Characteristics of Steel Slag for CO2 Capture. *Energy Fuels* **2011**, *25* (11), 5483−5492.

(20) Chang, E.-E.; Chen, C.-H.; Chen, Y.-H.; Pan, S.-Y.; Chiang, P.-C. Performance evaluation for carbonation of steel-making slags in a slurry reactor. *J. Hazard. Mater.* **2011**, *186* (1), 558−564.

(21) van Zomeren, A.; van der Laan, S. R.; Kobesen, H. B. A.; Huijgen, W. J. J.; Comans, R. N. J. Changes in mineralogical and leaching properties of converter steel slag resulting from accelerated carbonation at low CO2 pressure. *Waste Manage.* **2011**, *31* (11), 2236−2244.

(22) Hartmann, J.; West, A. J.; Renforth, P.; Köhler, P.; De La Rocha, C. L.; Wolf-Gladrow, D. A.; Dürr, H. H.; Scheffran, J. Enhanced chemical weathering as a geoengineering strategy to reduce atmospheric carbon dioxide, supply nutrients, and mitigate ocean acidification. *Rev. Geophys.* **2013**, *51* (2), 113−149.

(23) Schuiling, R. D.; Krijgsman, P. Enhanced weathering: An effective and cheap tool to sequester CO₂. *Clim. Change* **2006**, *74* (1−3), 349−354.

(24) Renforth, P.; Henderson, G. Assessing ocean alkalinity for carbon sequestration. *Rev. Geophys.* **2017**, *55* (3), 636−674.

(25) Fuss, S.; Canadell, J. G.; Peters, G. P.; Tavoni, M.; Andrew, R. M.; Ciais, P.; Jackson, R. B.; Jones, C. D.; Kraxner, F.; Nakicenovic, N.; et al. Betting on negative emissions. *Nat. Clim. Change* **2014**, *4*, 850.

(26) Edenhofer, O.; Pichs-Madruga, R.; Sokona, Y.; Farahani, E.; Kadner, S.; Seyboth, K.; Adler, A.; Baum, I.; Brunner, S.; Eickemeier, P.; Kriemann, B.; Savolainen, J.; Schlömer, S.; von Stechow, C.; Zwickel, T.; Minx, J. C., Eds. *Mitigation of climate change. Contribution of working group III to the fifth assessment report of the intergovernmental panel on climate change 5.*; Cambridge University Press: Cambridge, United Kingdom, 2014.

(27) Gasser, T.; Guivarch, C.; Tachiiri, K.; Jones, C. D.; Ciais, P. Negative emissions physically needed to keep global warming below 2 °C. *Nat. Commun.* **2015**, *6*, 7958.

(28) Gunning, P. J.; Hills, C. D.; Carey, P. J. Accelerated carbonation treatment of industrial wastes. *Waste Manage.* **2010**, *30* (6), 1081−1090.

(29) Wilson, S. A.; Dipple, G. M.; Power, I. A.; Thom, J. M.; Anderson, R. G.; Raudsepp, M.; Gabites, J. E.; Southam, G. Carbon dioxide fixation within mine wastes of ultramafic-hosted ore deposits: Examples from the Clinton Creek and Cassiar Chrysotile deposits, Canada. *Econ. Geol. Bull. Soc. Econ. Geol.* **2009**, *104* (1), 95−112.

(30) Renforth, P.; Manning, D. A. C.; Lopez-Capel, E. Carbonate precipitation in artificial soils as a sink for atmospheric carbon dioxide. *Appl. Geochem.* **2009**, *24* (9), 1757−1764.

(31) Washbourne, C.-L.; Renforth, P.; Manning, D. A. C. Investigating carbonate formation in urban soils as a method for capture and storage of atmospheric carbon. *Sci. Total Environ.* **2012**, *431* (C), 166−175.

(32) Environment Agency. *LIDAR Composite DSM - 2m. Environment Agency United Kingdom.* http://environment.data.gov.uk/discover/ea (accessed May 1, 2018).

(33) Parkhurst, D. L.; Appelo, C. *User's guide to PHREEQC (Version 2): A computer program for speciation, batch-reaction, onedimensional transport, and inverse geochemical calculations*; U.S. Geological Survey National Research Program Central Branch: Washington, DC, 1999.

(34) *Ordnance Survey.* Ordnance Survey (GB), Using: EDINA Digimap Ordnance Survey Service. http://digimap.edina.ac.uk (accessed October 12, 2017).

(35) Jenkins, W. *Consett Iron Works in 1893: A contemporary description of the steel and iron manufacturing carried on at Consett steelworks during the Victorian Era*; Ad Publishing: Hertfordshire, United Kingdom, 2008.

(36) Moore, T. *Consett: A Commemoration of The Works. The People's History*, 1st ed.; Seaham, Co.: Durham, United Kingdom, 2000.

(37) de Brito, J.; Saikia, N. Chapter 2: Industrial Waste Aggregates. In *Recycled Aggregate in Concrete*; Green Energy and Technology: New York, 2013; p 36.

(38) Proctor, D. M.; Fehling, K. A.; Shay, E. C.; Wittenborn, J. L.; Green, J. J.; Avent, C.; Bigham, R. D.; Connolly, M.; Lee, B.; Shepker, T. O.; et al. Physical and Chemical Characteristics of Blast Furnace, Basic Oxygen Furnace, and Electric Arc Furnace Steel Industry Slags. *Environ. Sci. Technol.* **2000**, *34* (8), 1576−1582.

(39) Butler, D. K. *Near-Surface Geophysics in series Investigations in Geophysics*; Society of Exploration Geophysicists: Tulsa, OK, 2005.

(40) Ford, D.; Williams, P. *Karst Hydrogeology and Geomorphology*; John Wiley & Sons Ltd: Chichester, United Kingdom, 2007.

(41) Gomes, H. I.; Rogerson, M.; Burke, I. T.; Stewart, D. I.; Mayes, W. M. Hydraulic and biotic impacts on neutralisation of high-pH waters. *Sci. Total Environ.* **2017**, *601−602* (C), 1271−1279.

(42) Hudson, J. D. Stable isotopes and limestone lithification. *J. Geol. Soc.* **1977**, *133* (6), 637.

(43) Macleod, G.; Fallick, A. E.; Hall, A. J. The mechanism of carbonate growth on concrete structures, as elucidated by carbon and oxygen isotope analyses. *Chem. Geol. Isot. Geosci. Sect.* **1991**, *86* (4), 335−343.

(44) Clark, I. D.; Fontes, J.-C.; Fritz, P. Stable isotope disequilibria in travertine from high pH waters: Laboratory investigations and field observations from Oman. *Geochim. Cosmochim. Acta* **1992**, *56* (5), 2041−2050.

(45) Wilson, S. A.; Barker, S. L. L.; Dipple, G. M.; Atudorei, V. Isotopic disequilibrium during uptake of atmospheric CO_2 into mine process waters: Implications for CO_2 sequestration. *Environ. Sci. Technol.* **2010**, *44* (24), 9522−9.

(46) Usdowski, E.; Hoefs, J. 13C/12C partitioning and kinetics of CO2 absorption by hydroxide buffer solutions. *Earth Planet. Sci. Lett.* **1986**, *80* (1), 130−134.

(47) Dietzel, M.; Usdowski, E.; Hoefs, J. Chemical and 13C/12C- and 18O/16O-isotope evolution of alkaline drainage waters and the precipitation of calcite. *Appl. Geochem.* **1992**, *7* (2), 177−184.

(48) Létolle, R.; Gégout, P.; Moranville-Regourd, M.; Gaveau, B. Carbon-13 and Oxygen-18 Mass Spectrometry as a Potential Tool for the Study of Carbonate Phases in Concretes. *J. Am. Ceram. Soc.* **1990**, *73* (12), 3617−3625.

(49) Andrews, J. E.; Gare, S. G.; Dennis, P. F. Unusual isotopic phenomena in Welsh quarry water and carbonate crusts. *Terra Nova* **1997**, *9* (2), 67−70.

(50) van Strydonck, M. J. Y.; Dupas, M.; Keppens, E. Isotopic Fractionation of Oxygen and Carbon in Lime Mortar Under Natural Environmental Conditions. *Radiocarbon* **1989**, *31* (3), 610−618.

(51) O'Neil, J. R.; Barnes, I. C13 and O18 compositions in some fresh-water carbonates associated with ultramafic rocks and serpentinites: western United States. *Geochim. Cosmochim. Acta* **1971**, *35* (7), 687−697.

(52) Younger, P. L. Hydrogeochemistry of minewaters flowing from abandoned coal workings in County Durham. *Q. J. Eng. Geol. Hydrogeol.* **1995**, *28* (2), S101−S113.

(53) Renforth, P.; Mayes, W. M.; Jarvis, A. P.; Burke, I. T.; Manning, D. A. C.; Gruiz, K. Contaminant mobility and carbon sequestration downstream of the Ajka (Hungary) red mud spill: The effects of gypsum dosing. *Sci. Total Environ..* **2012** *421*, 253−259.

(54) Roadcap, G. S.; Kelly, W. B.; Bethke, C. M. Geochemistry of extremely alkaline (pH > 12) ground water in slag fill aquifers. *Groundwater* **2005**, *43* (6), 806−816.

(55) Carpenter, A. *CO_2 abatement in the iron and steel industry*; IEA Clean Coal Centre: London, England, **2012**.

(56) Fischedick, M.; Roy, J.; Abdel-Aziz, A.; Acquaye, A.; Allwood, J. M.; Ceron, J.-P.; Geng, Y.; Kheshgi, H.; Lanza, A.; Perczyk, D.; et al.. Industry. In. *Climate Change 2014: Mitigation of Climate Change. Contribution of Working Group III to the Fifth Assessment Report of the Intergovernmental Panel on Climate Change*; Edenhofer, O.; Pichs-Madruga, R.; Sokona, Y.; Farahani, E.; Kadner, S.; Seyboth, K.; Adler, A.; Baum, I.; Brunner, S.; Eickemeier, P.; Kriemann, B.; Savolainen, J.; Schlömer, S.; von Stechow, C.; Zwickel, T.; Minx, J. C., Eds. 2014.

(57) United Nations. United Nations Framework Convention on Climate Change. https://unfccc.int/resource/docs/2015/cop21/eng/l09r01.pdf (accessed Feb 8, 2016).

(58) Boyd, R.; Stern, N.; Ward, B. *What will global annual emissions of greenhouse gases be in 2030, and will they be consistent with avoiding global warming of more than 2°C?*; Centre for Climate Change Economics and Policy and Grantham Research Institute on Climate Change and the Environment: London, England, 2015.

(59) PIRAMID Consortium. *Engineering guidelines for the passive remediation of acidic and/ or metalliferous mine drainage and similar wastewaters.*; European Commission 5th Framework RTD Project no. EVK1-CT-1999-000021 "Passive in-situ remediation of acidic mine/ industrial drainage" (PIRAMID); University of Newcastle upon Tyne: Newcastle upon Tyne, United Kingdom, 2003.

(60) Mayes, W. M.; Jarvis, A. P.; Aumônier, J. Preliminary evaluation of a constructed wetland for treating extremely alkaline (pH 12) steel slag drainage. *Water Sci. Technol.* **2009**, *59* (11), 2253−2263.

(61) Banks, M. K.; Schwab, A. P.; Alleman, J. E.; Hunter, J. G.; Hickey, J. C. *Constructed wetlands for the remediation of blast furnace slag leachates*; Report FHWA/IN/JTRP-2006/03; Joint Transportation Research Program: West Lafayette, IN, 2006.

(62) Teir, S.; Eloneva, S.; Fogelholm, C.-J.; Zevenhoven, R. Dissolution of steelmaking slags in acetic acid for precipitated calcium carbonate production. *Energy* **2007**, *32* (4), 528−539.

I